



Strong field evidence of directional permeability scale effect in fractured rock

Walter A. Illman^{1,*}

Department of Geoscience, University of Iowa, 121 Trowbridge Hall, Iowa City, IA 52242, USA

Received 30 August 2004; revised 21 January 2005; accepted 28 June 2005

Abstract

Permeability is a key parameter that controls mass and energy transport in geologic media. Its spatial variation is generally agreed within the research community, while the scale effect in permeability is still under considerable debate. This debate is mainly due to the lack of consistent measurement and interpretation of site data. Here, we show a strong field evidence of directional permeability scale effect from cross-hole pneumatic injection tests conducted in unsaturated fractured tuff at a field site in central Arizona, USA. The analysis reveals that permeability increases with the radial distance measured between the centroids of injection and monitoring locations of the test, which we consider to be the measurement scale. These results are compared to previously analyzed single-hole tests conducted at multiple measurement scales. We hypothesize that the permeability scale effect is controlled by the connectivity of fluid conducting fractures, which also increases with scale. This observation and hypothesis is consistent with existing scaling theories in fracture connectivity, although subsurface fracture connectivity cannot be measured directly with present technology. These results suggest the need to obtain permeability estimates that are commensurate with the scale of intended use.

© 2005 Elsevier Ltd All rights reserved.

Keywords: Permeability; Fractures; Tuff; Tomography; Unsaturated zone; Statistical analysis; Scale effect

1. Introduction

Permeability is a key parameter that controls fluid, solute, and energy transport in geologic media. Its magnitude and spatial distribution are important for all studies involving subsurface fluid migration. It can

additionally be useful inter alia in understanding large-scale geological processes such as earthquake occurrence (e.g. [Davies, 1999](#)), coseismic response of streamflow and water well responses ([Montgomery and Manga, 2003](#)), hydrothermal fluid circulation within the sea floor ([Fisher and Becker, 2000](#)), and volcanic eruptions ([Gonnermann and Manga, 2003](#)). Permeability is a difficult parameter to characterize properly because of the inherent spatial heterogeneity of geologic media.

The spatial dependence of permeability is widely accepted ([Gelhar 1993](#); [Dagan and Neuman, 1997](#);

* Corresponding author.

E-mail address: walter-illman@uiowa.edu

¹ Also at Department of Civil and Environmental Engineering as well as IHR-Hydroscience and Engineering, University of Iowa, Iowa City, IA 52242, USA.

Zhang, 2002) but the scale effect in permeability is still under considerable debate (Clauser, 1992; Zlotnik et al., 2000; Butler and Healey, 1998a, b; Hunt, 2003a, b; Neuman, 2003; Neuman and Di Federico, 2003). Fig. 1 shows the average values of permeabilities compiled from various laboratory to regional scale studies in fractured geologic media (Clauser, 1992; Rasmussen et al., 1993; Rovey and Cherkauer, 1995; Guzman et al., 1996; Hanor, 1993; Guimerà et al., 1995; Hsieh et al., 1985; Hsieh, 1998; Martínez-Landa et al., 2000; Illman and Neuman, 2003) showing a general increasing trend of permeability with measurement scale from the laboratory to the regional scale ($-2 < \log_{10} \text{ scale} < 3$) and its stabilization at larger scales ($\log_{10} \text{ scale} > 3$). There is considerable scatter in the data because of the inherent

variability in geologic media from one locality to the next. One could also question whether this observation is real or an artifact of experimental bias (Hsieh, 1998; Zlotnik et al., 2000) as these data come from a variety of techniques including laboratory methods, small- and large-scale well tests and the regional scale estimates mainly from the calibration of numerical ground water models. In fact, examples of permeability scale effect cited in the literature are due to the comparison of permeabilities obtained by different techniques. For example, laboratory tests on cores disregard fractures while localized well tests may not sample the features that control fluid migration on a larger scale. The comparison of small (single-hole) and large scale (cross-hole) well tests conducted in fractured rocks may also not be

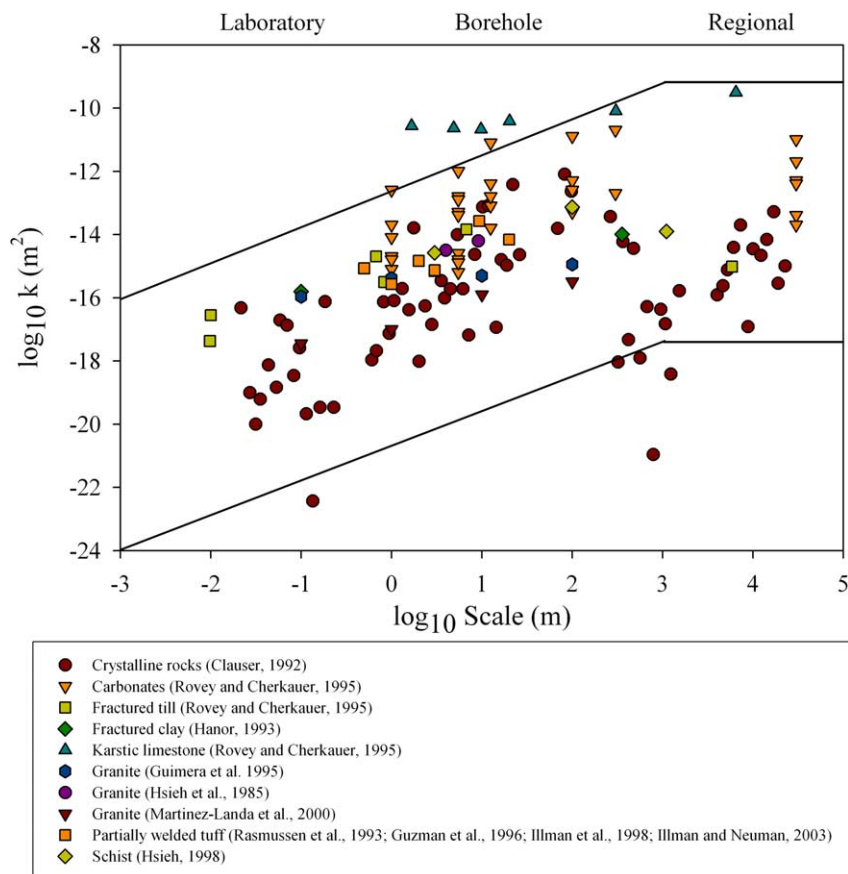


Fig. 1. Worldwide permeability (k) data plotted against measurement scale. The data are compiled for various fractured geologic media. A general increasing trend is observed for data in the range of $-2 < \log_{10} \text{ scale} < 3$. Permeability does not appear to increase further with scale beyond the regional scale ($\log_{10} \text{ scale} > 3$) for the available data.

always justified because the larger scale test may preferentially sample high conductivity features such as fractures and faults, while the small-scale tests may sample a combination of both the matrix and fractures. Likewise, larger scale fluid injection or pumping tests conducted in a single configuration (i.e. not in a tomographic manner) may miss the conductive properties of the rock at a given site leading to measurement bias.

There is currently no field data obtained by a single method that tests the rock at multiple scales from different directions that conclusively shows the variation of permeability with measurement scale. This is partly because of the difficulty in characterizing permeability at multiple scales with a consistent method. Therefore, the main objective of this paper is to show a strong field evidence of a directional permeability scale effect from multiple cross-hole pneumatic injection tests conducted in a tomographic manner in a geologically distinct unit of unsaturated fractured tuff.

2. Site and data description

The cross-hole pneumatic injection tests were conducted at the Apache Leap Research Site (ALRS) located in central Arizona, USA. The site included 22 vertical and inclined (at 45°) boreholes completed to a maximum vertical depth of 30 m in a geologically homogeneous mass of unsaturated fractured tuffaceous rock. Prior to the cross-hole tests, a large number of single-hole tests (Rasmussen et al., 1990; Rasmussen et al., 1993; Guzman et al., 1996; Illman et al., 1998) were conducted in a selected number of boreholes. During a single-hole test, air was injected into a borehole section isolated from the rest of the hole by inflatable packers. Among numerous single-hole tests, 184 were conducted (Guzman et al., 1996) in six boreholes (V2, W2A, X2, Y2, Y3, Z2) with a borehole interval length of 1.0 m. Tests were also conducted at multiple borehole interval lengths of 0.5, 1.0, 2.0, 3.0 and 20.0 m in one of the boreholes labeled Y2 (Guzman et al., 1996; Illman et al., 1998) located in the central portion of the studied rock mass. These single-hole tests were conducted to study the phenomenology of airflow

through fractures and spatial variability in hydrogeologic parameters at the site.

Permeabilities determined from single-hole tests represent the rock immediately surrounding the injection interval. As this does not provide information about the rock beyond the immediate vicinity of the injection interval, cross-hole tests were conducted to study the spatial and scale dependence of flow and transport parameters. The tests involved air injection into one isolated borehole interval while monitoring pressure simultaneously in numerous other such intervals within this and surrounding boreholes (Illman et al., 1998; Illman and Neuman, 2001, 2003; see also Illman, 1999). The injection and monitoring intervals were placed on fractures that were visible on available borehole television surveys. The locations of the intervals were also based on the available single-hole test data and the subsurface distribution of the permeabilities that were derived from the geostatistical analysis (Chen et al., 2000) of these small-scale measurements.

The tests were performed using modular straddle packer systems that were easily adapted to various test configurations and allowed rapid replacement of failed components, modification of the number of packers, and adjustment of distances between them in both the injection and monitoring boreholes. The main injection string consisted of three packers, one near the soil surface to isolate the borehole from the atmosphere, and two to enclose the injection interval. The air-filled volume of the injection interval was made relatively small so as to minimize borehole storage effects. Intervals with a single packer near the soil surface (of which we had six) are identified below by borehole designation; for example V1, X1, and W1. Where a modular system separates a borehole into three isolated intervals, we append to the borehole designation a suffix U, M, or B to identify the upper, middle, or bottom interval, respectively; for example V3U, V3M, and V3B. Where a modular system separates a borehole into four isolated intervals, we append to the borehole designation a suffix U, M, L, or B to identify the upper, middle, lower, or bottom interval, respectively; for example Z2U, Z2M, Z2L, and Z2B.

A typical cross-hole test consisted of packer inflation, a period of pressure recovery, air injection and another period of pressure recovery. Our system allowed rapid release of packer inflation pressure

when the corresponding recovery was slow, but this feature was never activated even though recovery had sometimes taken several hours. Once packer inflation pressure had dissipated in all (monitoring and injection) intervals, air injection at a constant flow rate began. It generally continued for several days until pressure in most monitoring intervals appeared to have stabilized. In some tests, injection pressure was allowed to dissipate until ambient conditions have been recovered. In other tests, air injection continued at incremental flow rates, each lasting until the corresponding pressure had stabilized, before the system was allowed to recover.

Three types of cross-hole tests were conducted at the ALRS in three phases. Phase 1 included line-injection/line-monitoring (LL) tests in which injection and monitoring took place along the entire length of a borehole that had been isolated from the atmosphere by means of shallow packers. Phase 2 consisted of point-injection/line-monitoring (PL) tests in which air was injected into a 2-m section in one borehole while pressure was recorded along the entire length of each monitoring borehole. During Phase 3, we conducted point-injection/point-monitoring (PP) tests in which the injection and a large number of monitoring intervals were short enough to be regarded, for

purposes of type-curve analysis (Illman and Neuman, 2001), as points. A total of 44 cross-hole pneumatic interference tests of various types (constant injection rate, multiple step injection rates, instantaneous injection) have been conducted using various configurations of injection and monitoring intervals (LL, PL, and PP) in 16 of the 22 boreholes, including the 11 subjected previously to single-hole tests.

A typical cross-hole test arrangement is shown in Fig. 2 in which the borehole locations, injection (larger colored spheres) and monitoring intervals (small black spheres) are depicted. Air injection took place in an interval (violet) located in borehole Y2 during cross-hole tests LL2, PL3, and PP4 (the number after the letter designation denotes the test number). Air injection also took place from different directions in discrete intervals of boreholes X2 (PP5, red sphere), Z3 (PP6, blue sphere), and W3 (PP7, yellow sphere). In fact, the cross-hole tests were conducted in a tomographic manner, meaning that air injection was done at a variety of locations throughout the rock mass, while pressure was recorded in surrounding monitoring intervals during each of these tests. This allowed for the testing of rock with different injection and observation configurations making them very unique in comparison to commonly

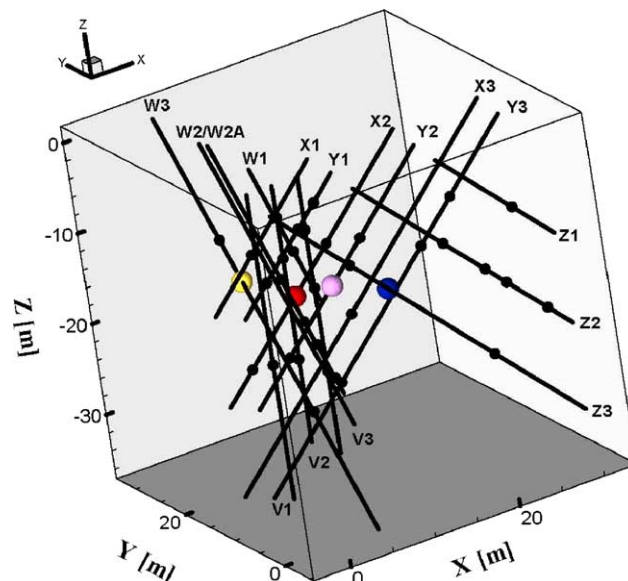


Fig. 2. Three-dimensional perspective view of boreholes (solid black lines), with centroids of injection (larger colored spheres) and observation intervals (small black spheres) shown for selected cross-hole tests at the ALRS (Fig. 3(a)–(f)).

executed pumping and injection tests in porous and fractured media. An additional unique aspect of these tests was that they were conducted at multiple scales.

Transient and steady-state analyses of these tests to date (Illman and Neuman, 2001, 2003; Vesselinov et al., 2001a, b) show that the permeability scale effect results from the comparison of single- and cross-hole test data and this can be explained theoretically by treating the permeability field as a self-affine random fractal (Hyun et al., 2002). However, there is considerable uncertainty whether the comparison of the data from the two types of tests really reveal a scale effect because the tests were conducted in a different configuration that could potentially introduce an experimental bias. The single-hole tests were conducted along the boreholes in 11 boreholes where the bulk of the rock is unfractured and so they will be representative of the combined properties of the fracture and rock matrix. Fracture porosity determined from cross-hole tests (Illman and Neuman, 2001; Illman and Tartakovsky, 2005) range between 10^{-5} and 10^{-2} which suggests that only a small portion of the rock conducts flow. Therefore, a ‘true’ permeability scale effect can only be measured from the comparison of permeabilities from a single type of test conducted over a large range of scales at various configurations. The cross-hole tests at the ALRS fit this criterion.

3. Steady-state analysis of cross-hole test data

The analyses of all analyzable cross-hole test data were performed with a fully three-dimensional analytical solution (Hsieh and Neuman, 1985) adapted for airflow conditions. The solution explicitly

$$k = \frac{Q\mu}{4\pi L\bar{p}} \times \frac{1}{2} \int_{\lambda=-1}^{\lambda=1} \ln \left[\frac{\{[(\alpha_1^2\lambda^2/\beta_1^2 + 2(\alpha_1^2\beta_2 + \alpha_1c)\lambda/\beta_1) + (\alpha_1^2 + 2\alpha_1\alpha_2 + 1)]^{1/2} + \alpha_1\alpha_2 + 1 + \alpha_1c\lambda/\beta_1\}}{\{[(\alpha_1^2\lambda^2/\beta_1^2 + 2(\alpha_1^2\beta_2 - \alpha_1c)\lambda/\beta_1) + (\alpha_1^2 - 2\alpha_1\alpha_2 + 1)]^{1/2} + \alpha_1\alpha_2 - 1 + \alpha_1c\lambda/\beta_1\}} \right] d\lambda \quad (3)$$

considers the variable lengths of injection and observation intervals and their angular dependence. We use the steady-state form of the point source solution

$$k = \frac{Q\mu}{4\pi R\bar{p}} \quad (1)$$

when the injection and monitoring intervals can be treated for purposes of analysis as points. Here, k is permeability, Q is the flow rate, μ is dynamic viscosity, R is the radial distance between the centroids of the injection and monitoring intervals, and \bar{p} is the average change in pressure in the monitoring interval.

When the injection interval can be treated as a point, but the monitoring interval has to be treated as a line of finite length for the purpose of the analysis, we must instead use the steady-state form of the point-injection/line-monitoring solution given as

$$k = \frac{Q\mu}{4\pi R\bar{p}} \times \frac{\beta_1}{2} \ln \frac{(\beta_1^2 + 2\beta_1\beta_2 + 1)^{1/2} + \beta_1\beta_2 + 1}{(\beta_1^2 - 2\beta_1\beta_2 + 1)^{1/2} + \beta_1\beta_2 - 1}. \quad (2)$$

Here, the parameters β_1 and β_2 describe the geometric relationships between the injection and monitoring intervals. For the isotropic case $\beta_1 = 2R/B$ where B is the length of the observation interval and $\beta_2 = \cos \theta_1$, where θ_1 is the angle in radians between a unit vector pointing from the centroid of the injection interval towards the centroid of the monitoring interval and a unit vector parallel to the monitoring interval during the test. Hsieh and Neuman (1985) found that when $\beta_1 \geq 5.0$, one could use Eq. (1) to obtain an estimate of permeability instead of Eq. (2) for the point-injection/line-monitoring case.

When both the injection and monitoring intervals have to be treated as lines of finite lengths for the purpose of the analysis, we instead use the steady-state form of the line-injection/line-monitoring solution given as

Similar to the previous case for the isotropic case, $\alpha_1 = 2R/L$ where L is the length of the injection interval and $\alpha_2 = \cos \theta_2$, where θ_2 is the angle given in radians between a unit vector pointing from the centroid of the injection interval towards the centroid of the monitoring interval and a unit vector parallel to the injection interval. Note that c has a similar meaning as α_2 and β_2

and is related to the angle between the injection and monitoring intervals.

The steady state analysis was conducted on tests deemed successful in that (1) they did not suffer from

significant equipment failure and (2) their flow conditions were relatively well controlled and stable. Illman and Neuman (2003) analyzed all PL and PP-series data that fit these criteria with Eqs. (1) and (2).

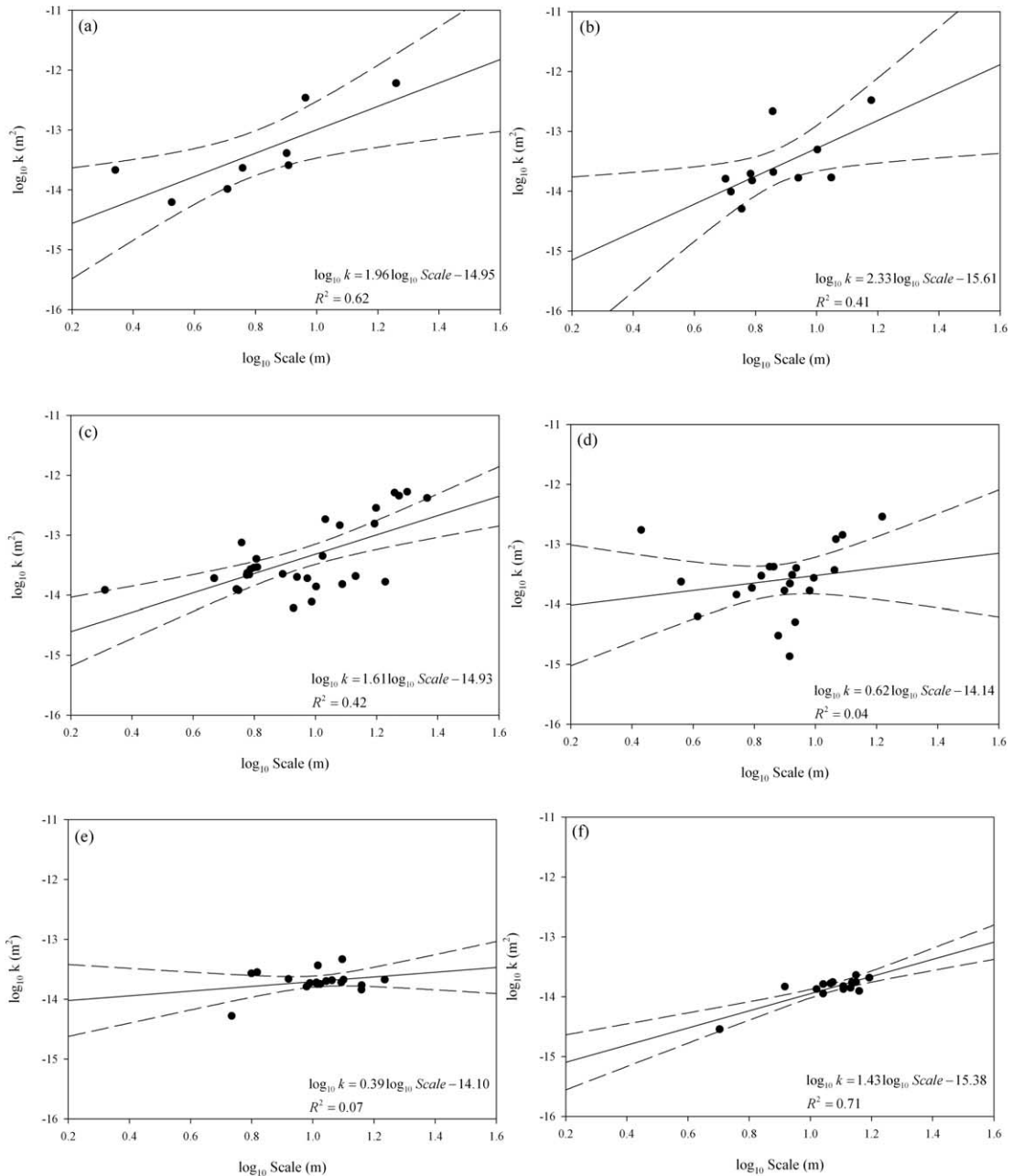


Fig. 3. (a)–(f) Plots of \log_{10} permeability (k) versus \log_{10} scale for six different cross-hole tests: (a) LL2, (b) PL3, (c) PP4, (d) PP5, (e) PP6, and (f) PP7 conducted at ALRS.

Here, we present the results from the steady-state analysis of test LL2, which required the use of Eq. (3) as well as previously obtained results from Illman and Neuman (2003).

The base 10 logarithm of permeabilities ($\log_{10} k$) from various cross-hole tests is plotted as solid circles in Fig. 3(a)–(f) against the base 10 logarithm of scale ($\log_{10} \text{scale}$). The scale here is defined as the radial distance between the centroids of the injection and the observation intervals during a given cross-hole test. The solid line is a linear model fit to the \log_{10} quantities with corresponding 95% confidence intervals shown as dashed curves.

We notice three key observations from the plots. First, we see that the values of permeability fluctuate erratically as the \log_{10} scale increases. This is because of the strong heterogeneous nature of the tested rock mass and that the permeabilities are determined for a volume smaller than the representative elementary volume (REV). Hydrogeologic parameters are known to fluctuate widely with support volume (scale) below

REV (Bear, 1972). However, one should note that for fractured geologic media a REV might not exist (Neuman, 1987) so that hydrogeologic parameters can vary with scale erratically, on all scales. Second, despite the scatter and varying quality of the fit of the linear model to the data, we see a general increasing trend in $\log_{10} k$ versus \log_{10} scale in most of the test results. This shows that there is a permeability scale effect obtained from a single-test type (i.e. cross-hole tests only) from multiple directions. Third, we see that the rate of increase in $\log_{10} k$ versus \log_{10} scale relationship varies from one test to the next, suggesting a directional effect in permeability scaling. In some tests, the scale effect is considerably stronger than others while in others, the scale effect is suppressed.

We next plot all cross-hole permeability data (open circles) together in Fig. 4 showing, on the whole, an increasing trend from 2–23 m (solid line). These data also suggest that two separate lines may be fit; one line (dashed) that shows that permeability increases with scale and the other (dotted) that suggests that

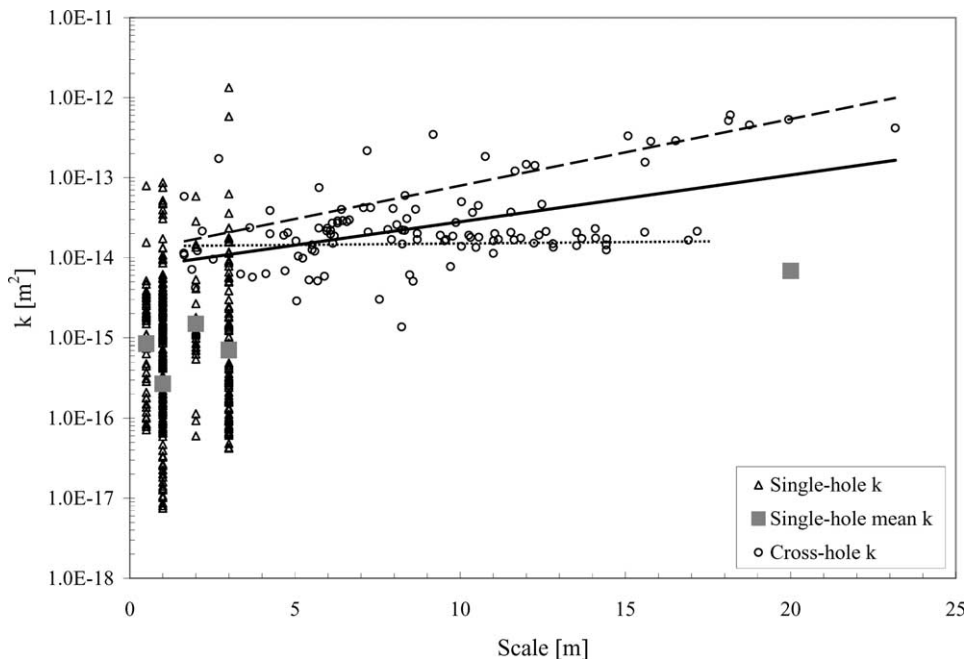


Fig. 4. Permeability (k) versus scale from single- and cross-hole pneumatic injection tests at the ALRS. Single-hole tests were conducted at five scales (0.5, 1.0, 2.0, 3.0, and 20 m) in borehole Y2, three scales (1.0, 2.0, and 3.0 m) in borehole X2, two scales (1.0 and 3.0 m) in boreholes Y3, Z2, and at 1 scale in boreholes V2 (1.0 m), W2A (1.0 m), X1 (3.0 m), X3 (3.0 m), Y1 (3.0 m), Z1 (3.0 m), and Z3 (3.0 m). Open triangles represent single-hole permeability values, solid squares denote the mean of single-hole permeability values at each scale, and open circles denote permeability estimates from cross-hole tests.

permeability does not vary with scale. This observation suggests that the permeability field at the ALRS determined from multiple cross-hole tests can be conceptualized as a multiscale stochastic continuum that exhibits directional random fractal behavior. In such a stochastic continuum, the permeability increases with scale directionally while in some directions the permeability increase is suppressed.

In Fig. 4, we also plot single-hole permeability data (open triangles) available at five different scales (0.5, 1.0, 2.0, 3.0, and 20.0 m) in 11 of the 16 boreholes used for cross-hole testing. For the single-hole data, the measurement scale is defined as the nominal length of the injection interval. The data show a very wide distribution at each scale, revealing the strongly heterogeneous nature of the rock at the site. Visual inspection of single-hole mean permeabilities (solid squares) from the 0.5–20.0 m shows a slight increasing trend, although one could equally argue that there is no scale effect in the single-hole permeabilities based on the available data. One could perhaps fit a model through the mean values computed at each scale, but we do not do this because only one permeability measurement is available at the 20-m scale in borehole Y2.

4. Discussion and concluding remarks

So what causes the directional permeability scale effect seen in the cross-hole test results? Explanations for the permeability scale effect posited include: (1) formation of skin around injection boreholes causing permeabilities obtained at the injection interval to be smaller than those determined in monitoring intervals (Butler and Healey, 1998a, b); (2) interpretation error arising from the use of inconsistent theory (Zlotnik et al., 2000); (3) dual nature of fractured rocks (Schulze-Makuch and Cherkauer, 1998); (4) use of data resulting from different measurement techniques (Hsieh, 1998; Zlotnik et al., 2000); (5) use of data from tests conducted over several formations (Rovey and Cherkauer, 1995); and (6) directional effects (Neuman and Di Federico, 2003).

The most likely cause of the scale effect due to the smearing and invasion of drilling fluids that cause artificially lower permeability estimates at the

injection well (i.e. the skin effect) is not the case here (Illman and Neuman, 2000). As for interpretation error, we relied on a single analytical technique and so there is consistency in the interpretation. It is also not due to the dual nature of the fractured rock, because fractures tend to be open to airflow under conditions of cross-hole tests at the site and the porous matrix is virtually saturated with water thus making it effectively impermeable to air. Airflow thus takes place exclusively in the fractures and the permeabilities reported here are representative of the fracture network only (Illman and Neuman, 2000, 2001). The tests have been conducted with a single consistent technique and so one can safely neglect the possibility of experimental bias. In addition, the tests have been conducted in a geologically homogenous block of rock negating the possibility of cross-flow among various units. The rock additionally has been tested from many different directions instead of a single configuration lending additional credence to these data and our interpretation. Although the magnitude of scaling differs from one direction to the next (Fig. 3(a)–(f)) because the rock is heterogeneous and the fractures clearly show a directional effect, these data for the first time shows the existence of a directional permeability scale effect over a measurement scale of 2–23 m (Fig. 3(a)–(f) and Fig. 4) and that the phenomenon is not a result of experimental or interpretive bias.

The cross-hole results demonstrate that the permeability scale effect is real and not an artifact but what is its real cause? Also, why does the rate of increase exhibit directional dependence? More importantly, does the permeability scale effect take place from the laboratory to the regional scales or beyond it as seen in Fig. 1?

We hypothesize that the permeability scale effect is controlled by the connectivity of fluid conducting fractures, which also increases with scale but varies directionally. In some terrains, the connectivity may decrease with scale, which should cause permeability to decrease with measurement scale. One can expect that fracture connectivity to be a directional quantity as fractures tend to be oriented in the direction of minimum principal stress. This explains why permeability does not increase significantly with the measurement scale for single-hole tests (Fig. 4) because these tests measure the rock properties in

the immediate vicinity of the injection interval at which fracture connectivity is limited (Illman, 2004). This additionally explains why permeability does not increase in a consistent fashion with direction as seen in Figs. 3(a)–(f) and perhaps at other localities where the permeability increase with measurement scale is limited (Hsieh, 1998) or is nonexistent.

This hypothesis is consistent with existing scaling theories in fracture connectivity (Bour and Davy, 1998; Darcel et al., 2003), although subsurface fracture connectivity in three-dimensions cannot be measured directly with present techniques without destroying the geologic medium. An indirect measure of fracture connectivity that should allow one to test this hypothesis could be obtained through the tomographic interpretation of geophysical and well test data (Yeh and Liu, 2000; Vesselinov et al., 2001a, b).

In any event, the strong field evidence of directional permeability scale effect shown here suggests that the parameter needs to be measured at the scale of its intended use for predictive studies of flow and transport in geologic media. However, such measurements are rarely available calling for new experimental and theoretical approaches that can capture multiscale variations in permeability and other hydrogeologic variables. In the absence of such measurements that are commensurate with the modeling scale, theoretical formulae that can up and downscale permeability could be used (Gelhar, 1993; Dagan and Neuman, 1997; Zhang, 2002), but the validation of such formulae with field data is very limited (Hyun et al., 2002). This study also calls for the development of new techniques to obtain permeability estimates and other fluid flow and transport parameters at widely varying scales. Research is also needed to quantify fracture connectivity better and relate this to spatial/scale dependence of permeability and other hydrogeologic parameters.

Acknowledgements

The author was supported in part by the 2003 Old Gold Fellowship from the University of Iowa, as well as by funding from the National Science Foundation (NSF) and the Strategic Environmental Research & Development Program (SERDP).

References

- Bear, J., 1972. Dynamics of Fluids in Porous Media. Dover Publications, Inc., New York.
- Bour, O., Davy, P., 1998. On the connectivity of three-dimensional fault networks. *Water Resour. Res.* 34, 2611–2622.
- Butler Jr., J.J., Healey, J.M., 1998. Relationship between pumping-test and slug-test parameters: scale effect or artifact? *Ground Water* 36, 305–313.
- Butler Jr., J.J., Healey, J.M., 1998. Discussion of papers: Authors' reply. *Ground Water* 36 (6), 867–868.
- Chen, G., Illman, W.A., Thompson, D.L., Vesselinov, V.V., Neuman, S.P., 2000. Geostatistical, type curve and inverse analyses of pneumatic injection tests in unsaturated fractured tuffs at the Apache Leap Research Site near Superior, AZ. In: Faybishenko, B. (Ed.), Dynamics of Fluids in Fractured Rocks Geophysical Monograph, vol. 122. AGU, Washington, DC, pp. 73–98.
- Clauser, C., 1992. Permeability of crystalline rocks. *Eos Trans., Am. Geophys. Union* 73, 233.
- Dagan, G., Neuman, S.P., 1997. Subsurface Flow and Transport: A Stochastic Approach. Cambridge University Press, Cambridge.
- Darcel, C., Bour, O., Davy, P., de Dreuzy, J.R., 2003. Connectivity properties of two-dimensional fracture networks with stochastic fractal correlation. *Water Resour. Res.* 39, 1272. doi:10.1029/2002WR001628.
- Davies, J.W., 1999. The role of hydraulic fractures and intermediate-depth earthquakes in generating subduction-zone magmatism. *Nature* 398, 142–145.
- Fisher, A.T., Becker, K., 2000. Channelized fluid flow in oceanic crust reconciles heat-flow and permeability data. *Nature* 403, 71–74.
- Gelhar, L.W., 1993. Stochastic Subsurface Hydrology. Prentice-Hall, Englewood Cliffs, NJ.
- Gonnermann, H.M., Manga, M., 2003. Explosive volcanism may not be an inevitable consequence of magma fragmentation. *Nature* 426, 432–435.
- Guimerà, J., Vives, L., Carrera, J., 1995. A discussion of scale effects on hydraulic conductivity at a granitic site (El Berrocal, Spain). *Geophys. Res. Lett.* 22, 1449–1452.
- Guzman, A.G., Geddis, A.M., Henrich, M.J., Lohrstorfer, C.F., Neuman, S.P., 1996. Summary of Air Permeability Data from Single-Hole Injection Tests in Unsaturated Fractured Tuffs at the Apache Leap Research Site: Results of Steady-State Test Interpretation, NUREG/CR-6360. US Nuclear Regulatory Commission, Washington, DC.
- Hanor, J.S., 1993. Effective hydraulic conductivity of fractured clay beds at a hazardous waste landfill, Louisiana Gulf Coast. *Water Resour. Res.* 29, 3691–3698.
- Hsieh, P.A., 1998. Scale effects in fluid flow through fractured geologic media. In: Sposito, G. (Ed.), Scale Dependence and Scale Invariance in Hydrology. Cambridge University Press, Cambridge, pp. 335–353.
- Hsieh, P.A., Neuman, S.P., 1985. Field determination of the three-dimensional hydraulic conductivity tensor of anisotropic media, 1. Theory. *Water Resour. Res.* 21, 1655–1665.

- Hsieh, P.A., Neuman, S.P., Stiles, G.K., Simpson, E.S., 1985. Field determination of the three-dimensional hydraulic conductivity tensor of anisotropic media. 2. Methodology and application to fractured rocks. *Water Resour. Res.* 21, 1667–1676.
- Hunt, A.G., 2003. Some comments on the scale dependence of the hydraulic conductivity in the presence of nested heterogeneity. *Adv. Water Resour.* 26, 71–77.
- Hunt, A.G., 2003. Reply to comment by S.P. Neuman on ‘some comments on the scale dependence of the hydraulic conductivity in the presence of nested heterogeneity’. *Adv. Water Resour.* 26, 1215.
- Hyun, Y., Neuman, S.P., Vesselinov, V.V., Illman, W.A., Tartakovsky, D.M., Di Federico, V., 2002. Theoretical interpretation of a pronounced permeability scale-effect in unsaturated fractured tuff. *Water Resour. Res.* 38. doi:10.1029/2001WR000658.
- Illman, W.A., 1999. Single- and cross-hole pneumatic injection tests in unsaturated fractured tuffs at the Apache Leap Research Site near Superior, AZ. PhD dissertation, Department of Hydrology and Water Resources, University of Arizona, Tucson.
- Illman, W.A., 2004. Analysis of permeability scaling within single boreholes. *Geophys. Res. Lett.* 31 (5), L06503. doi:10.1029/2003GL019303.
- Illman, W.A., Neuman, S.P., 2000. Type-curve interpretation of multi-rate single-hole pneumatic injection tests in unsaturated fractured rock. *Ground Water* 38, 899–911.
- Illman, W.A., Neuman, S.P., 2001. Type-curve interpretation of a cross-hole pneumatic injection test in unsaturated fractured tuff. *Water Resour. Res.* 37, 583–603.
- Illman, W.A., Neuman, S.P., 2003. Steady-state analyses of cross-hole pneumatic injection tests in unsaturated fractured tuff. *J. Hydrol.* 281, 36–54.
- Illman, W.A., Tartakovsky, D.M., 2005. Asymptotic analysis of three-dimensional pressure interference tests: point source solution. *Water Resour. Res.* 41, W01002. doi:10.1029/2004WR003431.
- Illman, W.A., Thompson, D.L., Vesselinov, V.V., Neuman, S.P., 1998. Single-Hole and Cross-Hole Pneumatic Tests in Unsaturated Fractured Tuffs at the Apache Leap Research Site: Phenomenology, Spatial Variability, Connectivity and Scale. Rep. NUREG/CR-5559. US Nuclear Regulatory Commission, Washington, DC.
- Martínez-Landa, L., Carrera, J., Guimerà, J., Vázquez-Suñé, E., Vives, L., Meier, P., 2000. Methodology for the hydraulic characterization of a granitic block. In: Stauffer, F., Kinzelbach, W., Kovar, K., Hoehn, E. (Eds.), *Calibration and Reliability in Groundwater Modeling; Coping with Uncertainty*, ModelCARE 99 IAHS Publication 265. IAHS Press, Wallingford, Oxfordshire, pp. 340–345.
- Montgomery, D.R., Manga, M., 2003. Streamflow and water well responses to earthquakes. *Science* 300, 2047–2049.
- Neuman, S.P., 1987. Stochastic Continuum Representation of Fractured Rock Permeability as an Alternative to the REV and Fracture Network Concepts 1987 (pp. 533–561, *Rock Mechanics: Proceedings of the 28th US Symposium, Tucson, AZ*, edited by I.W. Farmer, J.J.K. Daemen, C.S. Desai, C.E. Glass, S.P. Neuman, A.A. Balkema, Rotterdam, 1240 p., Also in pp. 331–362, *Groundwater Flow and Quality Modelling*, edited by E. Custodio, A. Gurgui, J.B. Lobo Ferreira, NATO ASI Series C, 224, D. Reidel, Dordrecht, Holland, 843 p., 1988).
- Neuman, S.P., 2003. Comment on ‘Some comments on the scale dependence of the hydraulic conductivity in the presence of nested heterogeneity’ by A.G. Hunt. *Adv. Water Resour.* 26, 1213.
- Neuman, S.P., Di Federico, V., 2003. Multifaceted nature of hydrogeologic scaling and its interpretation. *Rev. Geophys.* 41, 3/1014.
- Rasmussen, T.C., Evans, D.D., Sheets, P.J., Blanford, J.H., 1990. Unsaturated Fractured Rock Characterization Methods and Data Sets at the Apache Leap Tuff Site, NUREG/CR-5596. US Nuclear Regulatory Commission, Washington, DC.
- Rasmussen, T.C., Evans, D.D., Sheets, P.J., Blanford, J.H., 1993. Permeability of Apache Leap Tuff: Borehole and Core measurements using water and air. *Water Resour. Res.* 29, 1997–2006.
- Rovey II, C.W., Cherkauer, D.S., 1995. Scale dependency of hydraulic conductivity measurements. *Ground Water* 33, 769–780.
- Schulze-Makuch, D., Cherkauer, D.S., 1998. Variations in hydraulic conductivity with scale of measurements during aquifer tests in heterogeneous, porous carbonate rock. *Hydrogeol. J.* 6, 204–215.
- Vesselinov, V.V., Neuman, S.P., Illman, W.A., 2001a. Three-dimensional numerical inversion of pneumatic cross-hole tests in unsaturated fractured tuff: 1. Methodology and borehole effects. *Water Resour. Res.* 37, 3001–3018.
- Vesselinov, V.V., Neuman, S.P., Illman, W.A., 2001b. Three-dimensional numerical inversion of pneumatic cross-hole tests in unsaturated fractured tuff: 2. Equivalent parameters, high-resolution stochastic imaging and scale effects. *Water Resour. Res.* 37, 3019–3041.
- Yeh, T.-C.J., Liu, S., 2000. Hydraulic tomography: development of a new aquifer test method. *Water Resour. Res.* 36, 2095–2105.
- Zhang, D., 2002. *Stochastic Methods for Flow in Porous Media*. Academic Press, San Diego, CA.
- Zlotnik, V.A., Zurbuchen, B.R., Ptak, T., Teutsch, G., 2000. Support volume and scale effect in hydraulic conductivity: experimental aspects. In: Zhang, D., Winter, C.L. (Eds.), *Theory, Modeling, and Field Investigation in Hydrogeology: A Special Volume in Honor of Shlomo P. Neuman’s 60th Birthday*: Boulder, CO Geological Society of America Special Paper 348, pp. 191–213.